

## Toward Raman Fingerprints of Single Dye Molecules at Atomically Smooth Au(111)

Katrin F. Domke,\* Dai Zhang, and Bruno Pettinger

Contribution from the Fritz Haber Institute of the Max Planck Society, Faradayweg 4-6, 14195 Berlin, Germany

Received August 10, 2006; E-mail: domke@fhi-berlin.mpg.de

**Abstract:** The creation of a highly enhanced electromagnetic (EM) field underneath a scanning tunneling microscope (STM) tip enables Raman spectroscopic studies of organic submonolayer adsorbates at atomically smooth single crystalline surfaces. To study the sensitivity of this technique, tip-enhanced resonance Raman (TERR) spectra of the dye malachite green isothiocyanate on Au(111) in combination with the corresponding STM images of the probed surface region were analyzed. The detection limit for unambiguous identification of the dye and semiquantitative determination of the surface coverage reaches  $\leq 0.7$  pmol/cm<sup>2</sup>, or approximately five molecules present in the enhanced-field region, which is confirmed by STM images. Because of well-defined adsorption sites at atomically smooth Au(111) surfaces, no variation in band positions or relative band intensities was observed at the single- or few-molecule detection level when employing TERR spectroscopy.

### I. Introduction

Tip-enhanced Raman spectroscopy (TERS), also called apertureless scanning near-field optical microscopy (aSNOM), is a fairly young technique that combines Raman spectroscopy and scanning probe microscopy (SPM) to a spectroscopic–microscopic tool with hitherto unprecedented sensitivity and resolution. TERS permits to detect and identify a wide range of molecules with optically resonant or nonresonant transitions in the frequency region of the exciting laser line (in the following referred to as resonant and nonresonant molecules) adsorbed at atomically flat substrates. Raman studies at single crystalline samples even with submonolayer adsorbate concentrations have become an easy task.<sup>1,2</sup> To create the enormous electromagnetic (EM) field necessary for the detection of submonolayer adsorbates, the laser beam is focused onto a sharp metal tip. Because of the excitation of localized surface plasmons in the tip apex, the required near field is generated in the cavity between tip and sample. Only the molecules positioned in the enhanced-field (EF) region underneath the tip apex give rise to intense Raman bands.

Up to date, optical detection of single molecules (SM) is mainly carried out by fluorescence spectroscopy because of the relatively high photon count rates that can be reached.<sup>3–6</sup> However, the number of molecules with intrinsic fluorescence is limited, and the investigated species often has to be modified by a fluorescent moiety that acts as a “reporter”. The study of

single molecules by enhanced Raman spectroscopy is developing into an interesting alternative as it gives comparable photon count rates, allows the analysis of unmodified species, and provides more detailed information about molecular structure than fluorescence spectroscopy.<sup>7–13</sup>

The sensitivity of surface-enhanced Raman spectroscopy (SERS) has not been reached yet with TERS. Enhancement factors of up to  $10^{14}$  have been reported to be necessary for single-molecule (SM) detection with SERS. For TERS, maximum enhancement factors of  $6 \times 10^6$  have been achieved, which seems to be many orders of magnitude away from the SM detection limit.<sup>14,15</sup> However, TERS prevails over SERS, because the restriction of the latter to rough coinage metal surfaces as substrates is overcome.<sup>14</sup> In addition, the combination of SPM with Raman spectroscopy allows the correlation of topographic and chemical information at the nanometer scale. Generally, SPM techniques effortlessly facilitate molecular and atomic resolution, and the simultaneous chemical identification of the recorded structures has been a long-awaited goal in surface science.

In this work, we demonstrate the ability of tip-enhanced

- (1) Pettinger, B.; Ren, B.; Picardi, G.; Schuster, R.; Ertl, G. *Phys. Rev. Lett.* **2004**, *92*, 096101.
- (2) Ren, B.; Picardi, G.; Pettinger, B.; Schuster, R.; Ertl, G. *Angew. Chem., Int. Ed.* **2005**, *44*, 139.
- (3) Nie, S.; Zare, R. N. *Annu. Rev. Biophys. Biomol. Struct.* **1997**, *26*, 567.
- (4) Hess, S. T.; Huang, S.; Heikal, A. A.; Webb, W. W. *Biochemistry* **2002**, *41*, 697.
- (5) Bacia, K.; Kim, S. A.; Schwille, P. *Nat. Methods* **2006**, *3*, 83.
- (6) Myong, S.; Stevens, B. C.; Ha, T. *Structure* **2006**, *14*, 633.

- (7) Nie, S.; Emory, S. R. *Science* **1997**, *275*, 1102.
- (8) Kneipp, K.; Wang, Y.; Kneipp, H.; Perelman, L. T.; Itzkan, I.; Dasari, R. R.; Feld, M. S. *Phys. Rev. Lett.* **1997**, *78*, 1667.
- (9) Kneipp, K.; Kneipp, H.; Kartha, V. B.; Manoharan, R.; Deinum, G.; Itzkan, I.; Dasari, R. R.; Feld, M. S. *Phys. Rev. E* **1998**, *57*, R6281.
- (10) Michaels, A. M.; Nirmal, M.; Brus, L. *J. Am. Chem. Soc.* **1999**, *121*, 9932.
- (11) Neacsu, C. C.; Dreyer, J.; Behr, N.; Raschke, M. B. *Phys. Rev. B* **2006**, *73*, 193406.
- (12) Krug, J. T., II; Wang, G. D.; Emory, S. R.; Nie, S. *J. Am. Chem. Soc.* **1999**, *121*, 9208.
- (13) Habuchi, S.; Cotlet, M.; Gronheid, R.; Dirix, G.; Michiels, J.; Vanderleyden, J.; Schryver, F. C. D.; Hofkens, J. *J. Am. Chem. Soc.* **2003**, *125*, 8446.
- (14) Pettinger, B.; Ren, B.; Picardi, G.; Schuster, R.; Ertl, G. *J. Raman Spectrosc.* **2005**, *36*, 541.
- (15) In most single-molecule experiments, dyes are excited upon resonance conditions; hence, a resonance Raman scattering contribution of many orders of magnitude is included in the enhancement factor of  $10^{14}$ .

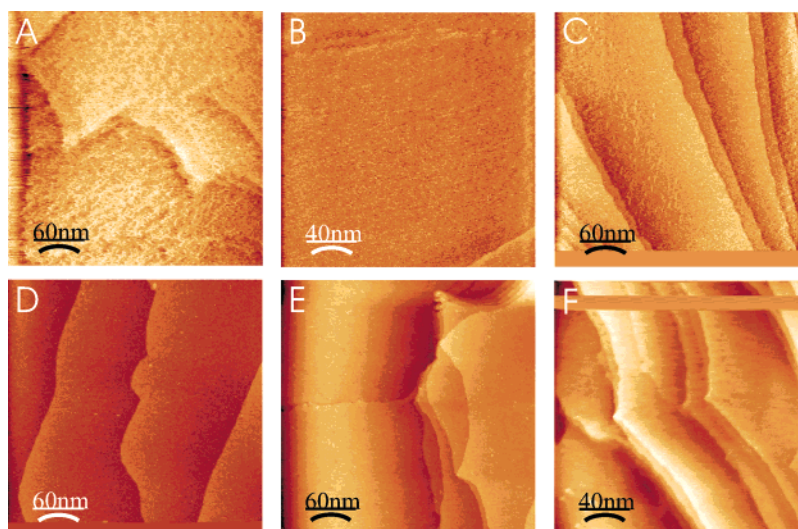


**Figure 1.** STM images of MGITC/Au(111) at different estimated adsorbate concentrations: (A) 170, (B) 73, (C) 33, (D) 24, (E) 1, and (F) 0.7 pmol/cm<sup>2</sup> (refer to discussion part for a detailed description of the determination of the surface coverages).  $U_{\text{bias}} = -100$  mV,  $I_t = 1$  nA, scan area as indicated.

resonance Raman (TERR) spectroscopy as a single-molecule analytical tool. Spectra of the triaryl dye malachite green isothiocyanate (MGITC) on Au(111) are investigated, where we make use of the additional resonance Raman enhancement of MGITC which has its absorption maximum centered at our excitation wavelength at 633 nm.<sup>15</sup> MGITC is adsorbed at a Au(111) single crystal from six differently concentrated solutions. In correlation with the corresponding STM images of the sample area, the sensitivity of TERRS as a probe for the detection and semiquantitative determination of the dye coverage is highlighted, indicating that we are approaching SM sensitivity with this technique.

## II. Experimental Section

Our TE(R)RS setup consists of a Raman spectrograph (LabRam 1000 from DILOR) which is controlled by Labspec 4.18 software (Jobin-Yvon) and is coupled to a home-built STM controlled by WSxM software (NanotecElectronic). All experiments are carried out in air. A red He–Ne laser beam (632.8 nm) is focused onto the STM Au-tip by a 50 $\times$  long working distance objective (numerical aperture, N.A. = 0.5) at an angle of 60 $^\circ$  of the optical axis to the surface normal with the polarization set to be parallel to the plane of incident (p-polarization). The incident power at the tip is 2 mW. If necessary, we employ gray filters to reduce the laser intensity to prevent the molecules from photobleaching. The spectral acquisition time varies between 1 and 20 s, depending on the incident laser power. All presented spectra are normalized to full power and 1-s integration time for better comparison.

The backscattered light is collected through the same objective, is led to the spectrometer (grating 600 L/mm), and is read out by a charge-coupled device (CCD) camera cooled with liquid nitrogen. The spectral resolution accomplished is 4 cm<sup>-1</sup>. Coarse approach of the tip and focusing of the laser beam are monitored with help of an additional CCD camera. Working in constant current mode at 1 nA, the tip is positioned approximately 1 nm above the sample. The bias voltage between tip and sample is set to -100 mV.

Pencil-shaped STM tips are produced from gold wire of 0.25-mm diameter by electrochemical etching in a 1:1 mixture of ethanol and fuming HCl.<sup>16</sup> We reproducibly obtain tip curvatures of 20 nm and, for these tips, assume the radius of the enhanced field to  $r_{\text{ef}} = 20$  nm according to a Heaviside step function approximation.

MGITC is purchased from Invitrogen and is dissolved in ethanol to give  $4.9 \times 10^{-5}$ ,  $1.2 \times 10^{-6}$ ,  $2.3 \times 10^{-7}$ ,  $1.2 \times 10^{-7}$ ,  $2.3 \times 10^{-8}$ , and  $1.2 \times 10^{-8}$  M solutions. The Au(111) single crystal (MaTeck) is flame-annealed according to the method of Clavilier<sup>17</sup> prior to MGITC adsorption to remove contaminations and obtain large, atomically smooth (111) terraces. After 1-h adsorption of MGITC from a continuously stirred 5-mL adsorption volume, the crystal is rinsed with 10 mL of ethanol to remove multilayers and is allowed to dry in air.

To rule out undesired contribution of surface-enhanced resonance Raman (SERR) scattering to the spectra, the tip is verified to be free of adsorbate after each TERR experiment. Even slight traces of contamination attached to an atomically rough tip can be easily observed because of intense SERR scattering from a retracted tip or a tip in tunneling contact with an adsorbate-free Au substrate. A spectrum of a clean tip (or negligibly contaminated) does not show any Raman bands.

Essential for obtaining a good TERR spectrum, and the main difficulty of the experiment, is precise focusing of the laser beam onto the tip apex. At the same time, the focusing time has to be reduced to a minimum to prevent photobleaching of the dye. For each concentration, several TERR spectra are recorded at different tip positions along the substrate surface to always guarantee a fresh, unbleached sample. At low dye concentrations, very few sample locations tested for TERR scattering lead to a reasonably intense and well-defined spectrum, because the statistical chance of “finding” an adsorbate molecule adds to the problems of degradation of the species and bad focusing. Only fingerprint spectra that exhibit the typical MGITC Raman features (and no carbon signals) are used for further analysis.

## III. Results

Figure 1 shows STM images of the Au(111) surface after adsorption of MGITC from differently concentrated solutions recorded in air. Figure 1A displays the substrate densely covered with adsorbate after 15-h adsorption from a  $1.2 \times 10^{-6}$  M solution. It is clearly seen that the MGITC molecules do not form a uniform and compact monolayer (ML) even after an extended adsorption time but give a rather irregular distribution of dotlike structures. Figure 1B–F displays a series of images recorded after 1-h adsorption time from increasingly diluted solutions ( $4.9 \times 10^{-5}$ ,  $2.3 \times 10^{-7}$ ,  $1.2 \times 10^{-7}$ ,  $2.3 \times 10^{-8}$ ,

(16) Ren, B.; Picardi, G.; Pettinger, B. *Rev. Sci. Instrum.* **2004**, *75*, 837.

(17) Clavilier, J.; Faure, R.; Guinet, G.; Durand, R. *J. Electroanal. Chem.* **1980**, *107*, 205.

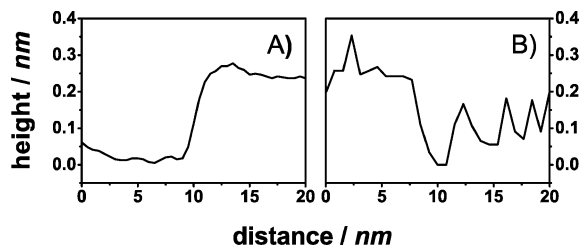


**Figure 2.** Typical STM line profiles for a Au(111) surface without/with MGITC adsorbate. (A) Atomically smooth (clean) Au(111) surface, Au step height approximately 0.24 nm. (B) The observed adsorbate structures appear of approximately 1.3–1.8 Å height and 1.5-nm diameter. A monatomic Au step of 0.24-nm height is clearly distinguishable from the nanodots.

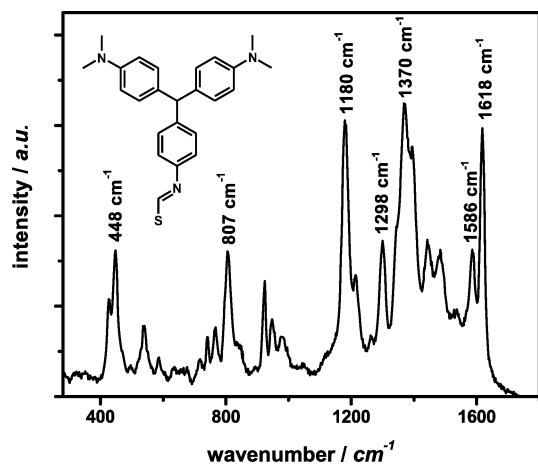


**Figure 3.** Inset: malachite green isothiocyanate (MGITC). Spectrum: TERS fingerprint of MGITC/Au(111) at high adsorbate concentration ( $\sim 100$  pmol/cm<sup>2</sup>). Laser power at sample: 2 mW, integration time: 1 s.

and  $1.2 \times 10^{-8}$  M, respectively). The images have been plane-flattened but have not been modified any further.

For Figure 1B–F, the number of adsorbates discernible in the images diminish with decreasing concentration. Size and geometry of the small, dotlike structures do not vary. At the highest investigated concentration, we find a densely covered Au surface after 1-h adsorption time; however, the adsorbate does not seem as tightly packed as in Figure 1A (15-h adsorption). At the lowest investigated concentration, the Au substrate seems smooth aside from monatomic steps in the substrate. No adsorbate molecules can be discerned in the image, and the few dots that should appear cannot be separated from noise.

To get a size estimate of the adsorbate structures seen in the images, we compare them to the monatomic steps of the substrate present in all images. Figure 2 shows two typical surface profiles for a clean, atomically smooth Au(111) surface (Figure 2A) and for Au(111) covered with MGITC (Figure 2B), respectively. The height of a Au step is found to be around 2.4 Å. The small structures are of approximately 1.5-nm diameter and appear visibly lower than the Au steps (around 1.3–1.8 Å). They do not form a densely packed monolayer but are separated by approximately 1–1.5 nm. Unfortunately, our experimental setup does not allow atomic or molecular resolution because of missing vibration and temperature isolation and thus aggravates the precise size analysis of the structures.

In Figure 3, a typical TERS spectrum of a monolayer MGITC adsorbed at a Au(111) substrate is shown. Its characteristic spectral features such as band positions and relative intensities

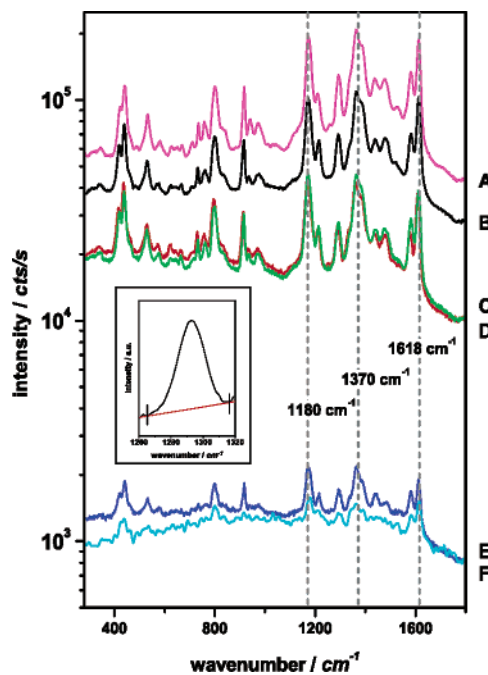


**Figure 4.** Average TERS spectra of MGITC/Au(111) at different adsorbate concentrations A–F, normalized to full laser power (2 mW at sample) and 1-s integration time. The inset shows an example of the straight baseline employed to obtain the Raman band intensity.

can be compared to spectra reported in the literature for MGITC in solution<sup>18</sup> and can allow the unambiguous identification of the triaryl dye. In the absence of the tip, no Raman bands are detectable (at short integration times). One of the advantages of carrying out Raman spectroscopy at metal substrates is that the fluorescence of the adsorbate is sufficiently quenched for Raman bands to be easily detected. The three most prominent bands appear at 1618, 1370 (with a shoulder at 1393 cm<sup>-1</sup>), and 1180 cm<sup>-1</sup>, in addition to several other characteristic features, like the strong bands at 1586, 807, and 448 cm<sup>-1</sup> (with a shoulder at 428 cm<sup>-1</sup>).

The corresponding six TERS spectra from MGITC/Au(111) at different surface coverages are plotted in a semilogarithmic plot in Figure 4. The spectra are averaged over five spectra recorded at different sample locations, and spectrum 4F has been smoothed to improve the signal-to-noise ratio. Interestingly, band and background intensities decrease collinearly. This is evident from Figure 4 by comparing the geometrical heights of the various peaks in curves A–D and the corresponding backgrounds. The band positions as well as the relative band intensities, however, do not change with the concentration. Even at very low surface concentrations of MGITC, the spectral characteristics allow an unequivocal identification of the molecule. All experimental spectra display a large background. No variation in band positions and relative band intensities between the individual spectra has been observed during the measurements.

#### IV. Discussion

The unique combination of microscopy and spectroscopy allows us to present a single-molecule study that confirms the (theoretically) estimated number of analyzed species with

(18) Lueck, H. B.; Daniel, D. C.; McHale, J. L. *J. Raman Spectrosc.* **1993**, *24*, 363.



topography images of the investigated sample area. To our knowledge, SM enhanced Raman studies have not yet employed SPM images to visualize the substrate and adsorbate geometry but usually rely on calculated molecule concentrations present in the probed volume.

In our recorded STM images, an apparent dependence of the surface coverage on the concentration of the adsorption solution is seen: Even for a high concentration of  $4.9 \times 10^{-5}$  M (which corresponds to an adsorbate concentration of  $2 \times 10^{16}$  molecules/cm<sup>2</sup> if all molecules from a 5-mL volume are adsorbed), completion of a ML cannot be observed after 1-h adsorption time. Kikteva et al. determined the maximum coverage of malachite green (MG), a similar dye lacking the SCN-group, to be  $1.6 \times 10^{14}$  molecules/cm<sup>2</sup> (one molecule occupying an area of approximately 60 Å<sup>2</sup>) on silica by optical second-harmonic generation experiments.<sup>19</sup>

At a first approximation, taking into account typical bond lengths, one MGITC molecule occupies a volume of  $1.2 \times 1 \times 0.2$  nm<sup>3</sup>. It is known from literature that MG adapts a slightly inclined orientation ( $\sim 55^\circ$ ) at silica or mica surfaces.<sup>19,20</sup> Hence, we assume a similarly tilted adsorption geometry for MGITC on gold, which is supported by the intense TERR spectra that are recorded. According to the surface selection rules, only vibrational modes with changes of polarization in  $z$ -direction perpendicular to the surface will be strongly enhanced.<sup>21</sup> For a  $55^\circ$ -inclined MGITC molecule, the surface area occupied amounts to approximately  $0.6 \times 1$  nm<sup>2</sup> according to the above-mentioned dimensions of the molecule. The structures found in the STM images are somewhat larger than expected for single MGITC molecules. This is attributed to the suboptimal lateral resolution of our instrument. There is no indication of agglomeration of dye molecules at low surface concentrations (Figure 1E,F). Although single dye molecules are not discernible from the noise in these images, a cluster of  $\geq 5$  nm diameter consisting of about five or more molecules would be clearly distinguishable.

MGITC is known to bind strongly to gold via the sulfur atom of its isothiocyanate group (see inset of Figure 3). Therefore, it is quite immobilized and stable on the substrate surface during the duration of the STM and Raman experiments, even when working in air. However, despite the chemical S–Au bond, surface diffusion of the molecules at room temperature cannot be ruled out. Supplementary experiments performed upon UHV conditions with a high-resolution STM did not produce better images. Cooling down the system to 200 K might help to improve the resolution and enable to monitor single MGITC molecules in detail. This work is in progress and will be published elsewhere.

It was very difficult to obtain STM images from the surfaces covered most densely with MGITC because of the high resistivity of the adsorbate. A similar attempt by Möltgen and Kleinermanns to obtain good-resolution STM images of MG on graphite also failed because of the small electrical conductivity of the adsorbate.<sup>22</sup> As the tunneling current perceives the high resistivity of the molecule, the tip approaches further. Thus,

we measure a small effective height of 0.2 nm, although an inclined MGITC molecule sticks out approximately 1 nm from the surface.

We conclude that the observed structures represent single MGITC molecules. The medium distance between the clusters is in the range of the cluster size which results in a medium area of around 100 Å<sup>2</sup> per MGITC molecule or  $1 \times 10^{14}$  molecules/cm<sup>2</sup>, a slightly lower ML coverage than estimated by Kikteva et al. for MG at silica.<sup>19</sup> The actual surface concentration could not be directly determined up to now, for instance, from fluorescence spectroscopy of re-desorbed species, because it was below the detection limit.

Figure 3 shows a typical fingerprint TERR spectrum of MGITC which allows us to unambiguously identify the adsorbate. Three prominent bands at 1618, 1586, and 1370 cm<sup>-1</sup> (with a shoulder at 1393 cm<sup>-1</sup>) are assigned to phenyl-N stretch and to the ring breathing and stretching of the aromatic ring according to Lueck et al.<sup>18</sup> In Figure 4, an overview of the TERR spectra recorded at different adsorbate coverages shows that a fingerprint of MGITC is obtained even for a very low number of scatterers. The recorded normalized and averaged TERR spectra in Figure 4 equally decrease in band and background intensities with decreasing concentration. As no band shifts or changes in relative band intensities are observed with variation of the adsorbate concentration, we conclude that neither the orientation of the molecules with respect to the surface nor the interaction between the adsorbed molecules vary substantially with the surface coverage and thus are negligible for the resulting Raman spectra. Even at the lowest investigated surface concentration, contamination of the sample does not cause problems, although the experiments are performed in air.

Spectral intensity and quality are found to vary largely from sample location to sample location. At every concentration and sample location, our aim was to obtain maximum signal intensity of the MGITC fingerprint. The main challenge is to perfectly focus the laser beam onto the tip apex. Only maximum energy transfer from the beam to the gold tip leads to an intense Raman spectrum. At low coverage, however, it is impossible to distinguish whether low scattering intensities are due to bad focusing or simply to the lack of target species beneath the tip. Another obstacle consists of the quick photobleaching of the dye.<sup>14</sup> Some of the recorded spectra (not shown here) exhibit pronounced peaks resembling carbon contamination resulting from the decomposition of MGITC, which do not allow a clear identification of the target species. As a consequence, we only analyze the TERR spectra of maximum signal intensity that exhibit the characteristic MGITC Raman bands.

The concentration of the solution cannot be related directly to the adsorbate concentration at the surface, although we find roughly a factor of 10 less TERR spectral intensity when decreasing the adsorbate solution concentration by 1 order of magnitude from  $10^{-7}$  to  $10^{-8}$  M (compare Figure 4). In general, this relation will, among other factors, depend on the substrate geometry, the surface diffusion of the molecules, and the concentration itself. It has been shown in concentration-dependent SERS studies that linearity between Raman intensity and solution concentration is given only for very low concentra-

(19) Kikteva, T.; Star, D.; Leach, G. *J. Phys. Chem. B* **2000**, *104*, 2860.

(20) Fischer, D.; Caseri, W.; Hähner, G. *J. Colloid Interface Sci.* **1998**, *198*, 337.

(21) Moskovits, M.; DiLella, D.; Maynard, K. *Langmuir* **1987**, *4*, 67.

(22) Möltgen, H.; Kleinermanns, K. *Phys. Chem. Chem. Phys.* **2003**, *5*, 2643.

**Table 1.** An Overview on the Integrated Spectral Intensities ( $I$ ) and the Corresponding Calculated Numbers of Scatterers in the Enhanced-Field Region (sc/ef) for the Differently Concentrated Adsorption Solutions A–F

analyzed band		A	B	C	D	E	F
100–1800 $\text{cm}^{-1}$	$I$ [cts/s]	$1.2 \times 10^{-6} \text{ M}^a$	$4.9 \times 10^{-5} \text{ M}$	$2.3 \times 10^{-7} \text{ M}$	$1.2 \times 10^{-7} \text{ M}$	$2.3 \times 10^{-8} \text{ M}$	$1.2 \times 10^{-8} \text{ M}$
	sc/ef	$1.32 \times 10^8$	$8.02 \times 10^7$	$3.55 \times 10^7$	$3.46 \times 10^7$	$2.28 \times 10^6$	$1.89 \times 10^6$
1298 $\text{cm}^{-1}$	$I$ [cts/s]	1257	764	338	330	22	18
	sc/ef	$9.84 \times 10^5$	$4.90 \times 10^5$	$1.94 \times 10^5$	$1.66 \times 10^5$	$6.33 \times 10^3$	$3.80 \times 10^3$
1586 $\text{cm}^{-1}$	$I$ [cts/s]	1257	626	248	212	8	5
	sc/ef	$1.32 \times 10^6$	$5.80 \times 10^5$	$2.74 \times 10^5$	$1.91 \times 10^5$	$9.80 \times 10^3$	$5.40 \times 10^3$
1618 $\text{cm}^{-1}$	$I$ [cts/s]	1257	552	261	182	9	5
	sc/ef	$2.34 \times 10^6$	$1.26 \times 10^6$	$4.58 \times 10^5$	$4.33 \times 10^5$	$1.46 \times 10^4$	$1.04 \times 10^4$
		1257	677	261	233	9	6

<sup>a</sup> Fifteen-hour adsorption time.

tions ( $10^{-9}$ – $10^{-7}$  M).<sup>23–25</sup> As can be seen from our experiment, the adsorption time also plays a crucial role.

In fact, the only linear indicator for the surface coverage and, thus, the number of Raman scatterers is the Raman band intensity that is measured. As we do not approach the saturated absorption regime, it is reasonable to expect a linear relationship between the number of Raman scatterers present at the Au(111) surface and the Raman band intensity.

To calculate the number of scatterers at each surface concentration, we take into account the maximum coverage and the corresponding spectral intensity, following the linear dependence of the TERR band intensity on the surface concentration of MGITC. To obtain the Raman band intensities, a straight baseline is set at the bottom of the Raman band and is integrated between the intersects of baseline and band feet, as shown in the inset of Figure 4. The area of the enhanced field is estimated to  $A_{\text{ef}} = \pi r_{\text{ef}}^2 = 1257 \text{ nm}^2$  with, at Heaviside approximation,  $r_{\text{ef}} = 20 \text{ nm}$ . Comparing the size of an MGITC molecule with the structures found in our STM images, we estimate that one molecule occupies approximately  $1 \text{ nm}^2$ . Thus, we presume a highest surface coverage  $N_A$  of  $1 \times 10^{14}$  molecules/ $\text{cm}^2$ , which corresponds to around 1260 molecules present in the EF region at maximum coverage.

We analyze the intensities of three different MGITC bands (deliberately chosen) at 1298, 1586, and 1618  $\text{cm}^{-1}$  as well as the total spectral intensity between 100 and 1800  $\text{cm}^{-1}$  to determine the number of resonant Raman scatterers present in the EF. According to  $(I_A/N_A) = (I_X/N_X)$ , we calculate the number of scatterers  $N_X$  present for different concentrations  $X$  from the integrated intensities  $I_X$ . For example, the 1298  $\text{cm}^{-1}$  band gives a total intensity  $I_A$  of  $9.84 \times 10^5$  cts/s for the highest adsorbate concentration  $N_A$ , or 783 cts/s per molecule, and consequently, we calculate that only five molecules are present in the enhanced field at the lowest concentration. Table 1 contains an overview for the series of experiments with different concentrations of MGITC.

For  $2.3 \times 10^{-7} \text{ M}$  ( $2.3 \times 10^{-8} \text{ M}$ ) solutions, we calculate an average number of scatterers of 248, 261, 261, and 338 (8, 9, 9, and 22) for the different MGITC bands and the background, respectively. For the lowest adsorbate concentration investigated in this study, this calculation leads to remarkably low numbers of 5, 6, 6, and 18 MGITC molecules detected with TERRS. Considering the topographic information obtained from STM

and the Raman band intensities, which are unquestionably due to inelastic scattering of the adsorbate, it is evident that the sensitivity reached with TERRS has approached the SM detection level!

The measured band intensities of the three bands give similar number of scatterers for all measured solution concentrations, whereas the integration of the total spectral intensity leads to a slightly higher number. This may be due to the fact that there are indeed some small contributions from contamination or from weak luminescence of the metal substrate itself. The discrepancies are quite small, however, and the comparison underlines the potential of TERRS as an SM analytical tool.

In addition, our calculation has the tendency to yield too large a number of scatterers. The real number of scatterers is likely to be smaller for two reasons:

(1) According to theory, the effective TE(R)R radius (i.e., the radius of the surface area from which 63% of the signal originates) is somewhat smaller than the curvature of the tip and the enhanced field radius.<sup>14,26</sup> Approximating the distribution of the enhanced field by a Gaussian profile, the TE(R)RS radius is half the field radius ( $r_{\text{TE(R)RS}} \sim 1/2 r_{\text{ef}}$ ), reaching a lateral resolution of 10 nm.<sup>14</sup> According to Rendell et al.,<sup>26</sup> the localization length of the field is  $(2r_{\text{tip}}d)^{1/2} = 7 \text{ nm}$  for a tip radius of 20 nm and a tunneling distance of  $d = 1 \text{ nm}$ , while eq A15 in ref 14 yields 9 nm. The lateral resolution is then twice these values, 14 and 18 nm, respectively. Recalculating the number of scatterers with  $r_{\text{ef}} \leq 1/2 r_{\text{tip}}$ , that is, with the theoretical estimations of the area from which the Raman scattering stems, we arrive at one single molecule. However, as these relations have not been proven experimentally, we prefer to (more safely) approximate  $r_{\text{TE(R)RS}} = r_{\text{ef}} = r_{\text{tip}}$ .

(2) Besides, it has been shown that the scattering intensity per molecule is smaller for a densely packed dye layer because of resonant absorption than for lower adsorbate concentrations, varying inversely with the square root of the number of molecules:  $I_{\text{ERS}}/n \approx n^{-1/2}$ .<sup>27</sup> This means that decreasing the surface coverage by 2 orders of magnitude from 1000 to 10 molecules leads to roughly a factor 10 more scattering intensity per molecule. Therefore, the alleged scattering rates per molecule should be corrected for lower adsorbate concentrations in the presented case. As a result, the real number of scatterers is expected to be clearly smaller than stated above, in fact reaching the SM level, where only one molecule is present in the EF region.

(23) Shadi, I. T.; Chowdhry, B. Z.; Snowden, M. J.; Withnall, R. *Appl. Spectrosc.* **2000**, *54*, 384.

(24) Shadi, I. T.; Chowdhry, B. Z.; Snowden, M. J.; Withnall, R. *Anal. Chim. Acta* **2001**, *450*, 115.

(25) McLaughlin, C.; Graham, D.; Smith, W. *J. Phys. Chem. B* **2002**, *106*, 5408.

(26) Rendell, R.; Scalapino, D.; Mühlenschlegel, B. *Phys. Rev. Lett.* **1978**, *41*, 1746.

(27) Pettinger, B.; Krischer, K.; Ertl, G. *Chem. Phys. Lett.* **1988**, *151*, 151.

It is often stated in the literature that an enhancement of  $10^{14}$  or  $10^{15}$  is needed to explain SM SERS.<sup>7,9</sup> However, the degree of electromagnetic and resonance enhancement should be discussed. Typical cross sections of normal Raman scattering for small, nonresonant molecules such as water lie in the range of  $10^{-30}$  cm<sup>2</sup>. For the usually employed, much larger dye molecules, we can expect an increase of a few orders of magnitude to  $\sim 10^{-28}$  cm<sup>2</sup>. In addition, resonance enhancement of the adsorbate plays a significant role and further increases the cross section.<sup>7,28,29</sup> In this context, most SM SE(R)RS experiments involve resonantly excited molecules.<sup>7,12,13,25,37,38</sup> A reasonable effective cross section for a resonant dye would then lie around  $10^{-23}$  cm<sup>2</sup>. To reach the SM detection level of around  $10^{-16}$  cm<sup>2</sup>, an additional electromagnetic enhancement of 7 orders of magnitude thus is sufficient. This has been reached with TERRS, as shown in ref 14, and indirectly with the high sensitivity in this report. Hence, single molecules can be detected with TERRS.

Often, SM SE(R)RS studies report of a “blinking” phenomenon.<sup>7,10,30</sup> Nie and Emory state that Raman signals suddenly disappear or change after a few minutes of continuous illumination, which suggests that each molecule is adsorbed at a different site (on a rough surface).<sup>7</sup> Michaels et al. find an “on/off behavior” of the investigated silver colloids as well as variations in the integrated intensities and slight band shifts of Rhodamine 6G.<sup>10</sup> The blinking is attributed to thermally driven desorption and readsorption of the molecules.

In our case, we do not find any blinking of the TERR spectra, even for the lowest adsorbate concentrations. This is in agreement with results from Hartschuh et al., who did not observe blinking behavior for TER spectra of carbon nanotubes on glass.<sup>31</sup> The main difference between SERRS and TERRS lies in the fact that the latter is carried out on smooth, single crystal surfaces. This means that, in principle, all adsorption sites for MGITC are spectroscopically equal, and molecular diffusion will not lead to changes in the spectra as long as the molecules stay in the EF region.

One of the main difficulties that occur upon the given experimental conditions is the photobleaching of the triaryl dye.<sup>1,14</sup> Especially when exposed to strong EM fields or laser light (absorption maximum at 630 cm<sup>-1</sup>), the molecules are likely to decompose quickly. It is indispensable to regularly move to fresh surface areas where no photobleaching has taken place to obtain satisfactory TERR spectra, and spectral integration time as well as the incident laser power have to be adjusted, respectively.

A similar SM study was performed by Neacsu et al. for MG on evaporated Au films.<sup>11</sup> However, they do not obtain

fingerprint spectra of the adsorbate at SM concentration, which would allow clear identification of the molecule. Exposing the sample to strong long-time illumination, it is likely that the dye is photobleached and that the spectra then show carbonaceous contamination (see ref 32 for discussion on the contamination problem in SM SERS).

The origin of the background, which is commonly observed in TE(R)R and SE(R)R spectra, is still under discussion, and spectra are therefore often presented after background correction in the literature (e.g., refs 7–9, 14). It was proposed by Otto et al. that the background is a byproduct of a nonradiative charge-transfer process between surface and molecule, an electron–hole pair formation and recombination.<sup>33</sup> In a more recent publication, Jiang et al. attributed the background to Ag electronic Raman scattering caused by an adsorbed dye exchanging electrons with the substrate.<sup>34</sup> Xu et al. and Johansson et al. carried out a density matrix calculation of surface-enhanced resonant Raman scattering and fluorescence of a molecule trapped between two silver spheres, discussing the influence of the field enhancement on these processes. Both are surface-enhanced, but to a different degree, which results in a structured fluorescence background underneath the Raman bands.<sup>35,36</sup>

Weiss and Haran report on a connection between background and Raman band intensity in their spectra.<sup>37</sup> They show that the background exists only in the presence of the spectrum and vice versa. A similar association of SER scattering and background continuum was found by Moore et al.<sup>38</sup> As we observe a linear decrease of the background with the Raman scattering intensity (and thus with the surface coverage), we conclude (1) that the background mainly stems from the adsorbate (or an adsorbate–metal complex) and represents most likely enhanced fluorescence and (2) that contributions from the substrate and contaminations are negligible in a first approximation when working with resonant Raman scatterers.

It would be interesting to carry out TER studies on a pure Au(111) surface working in an inert gas atmosphere to investigate possible spectral contributions from the substrate. With the current setup, experiments with a supposedly “clean” gold substrate will always show Raman bands and a fluorescent-like background continuum resulting from unknown contamination. For the recorded TERR spectra from Au covered with adsorbate, however, the contamination bands are of negligible significance, because the resonantly enhanced bands of MGITC (as well as the enhanced fluorescence background) always appear much stronger.

## V. Conclusions

In summary, combining spectroscopy and microscopy at nanometer scale, TE(R)RS is becoming an interesting SM analysis tool that could provide also promising advantages for the ultrasensitive characterization of biophysically relevant species. For the first time, an SM TERR study provides visual evidence for an extremely low concentration of the investigated dye, providing a sensible basis for SM investigation. We have shown that MGITC adsorbed at a single crystalline Au(111) surface can be analyzed easily down to 0.7 pmol/cm<sup>2</sup> or to around five molecules present in the EF region, giving rise to a fingerprint spectrum even at lowest surface coverage. This means that, at present, with a moderate enhancement of about  $10^6$ – $10^7$ , our spectral sensitivity is less than 1 order of magni-

- (28) Haslett, T.; Tay, L.; Moskovits, M. *J. Chem. Phys.* **2000**, *113*, 1641.  
(29) Zhao, L.; Jensen, L.; Schatz, G. C. *J. Am. Chem. Soc.* **2006**, *128*, 2911.  
(30) Moyer, P. J.; Schmidt, J.; Eng, L. M.; Meixner, A. *J. Am. Chem. Soc.* **2000**, *122*, 5409.  
(31) Hartschuh, A.; Pedrosa, H. N.; Novotny, L.; Krauss, T. D. *Science* **2003**, *301*, 1354.  
(32) Otto, A. *J. Raman Spectrosc.* **2002**, *33*, 593.  
(33) Otto, A.; Mrozek, L.; Grubhorn, H.; Akemann, W. *J. Phys.: Condens. Matter* **1992**, *4*, 1143.  
(34) Jiang, J.; Bosnick, K.; Maillard, M.; Brus, L. *J. Phys. Chem. B* **2003**, *107*, 9964.  
(35) Xu, H.; Wang, X.-H.; Persson, M. R.; Xu, H.; Käll, M.; Johansson, P. *Phys. Rev. Lett.* **2004**, *93*, 243002.  
(36) Johansson, P.; Xu, H.; Käll, M. *Phys. Rev. B* **2005**, *72*, 035427.  
(37) Weiss, A.; Haran, G. *J. Phys. Chem. B* **2001**, *105*, 12348.  
(38) Moore, A. A.; Jacobson, M. L.; Belabas, N.; Rowlen, K. L.; Jonas, D. M. *J. Am. Chem. Soc.* **2005**, *127*, 7292.

tude away from the SM detection level. From the recorded STM images, we find that MGITC does not form a densely packed monolayer on Au(111) upon our experimental conditions. Despite the suboptimal resolution, single MGITC molecules are discernible in the images in form of  $\sim 1$  nm sized dots.

**Acknowledgment.** The authors thank Prof. Konrad Weil for helpful discussions and thorough proofreading of the manuscript. D.Z. gratefully acknowledges a Max Planck fellowship.

JA065820B